

Power and Propulsion System Design for Near-Earth Object Robotic Exploration

John Steven Snyder,^{*} Thomas M. Randolph,[†] and Damon F. Landau[‡]
Jet Propulsion Laboratory, California Institute of Technology, Pasadena, CA, 91109

and

Kristen M. Bury,[§] Shane P. Malone,^{**} and Tyler A. Hickman^{††}
NASA Glenn Research Center, Cleveland, OH, 44135

Near-Earth Objects (NEOs) are exciting targets for exploration; they are relatively easy to reach but relatively little is known about them. With solar electric propulsion, a vast number of interesting NEOs can be reached within a few years and with extensive flexibility in launch date. An additional advantage of electric propulsion for these missions is that a spacecraft can be small, enabling a fleet of explorers launched on a single vehicle or as secondary payloads. Commercial, flight-proven Hall thruster systems have great appeal based on their performance and low cost risk, but one issue with these systems is that the power processing units (PPUs) are designed for regulated spacecraft power architectures which are not attractive for small NEO missions. In this study we consider the integrated design of power and propulsion systems that utilize the capabilities of existing PPUs in an unregulated power architecture. Models for solar array and engine performance are combined with low-thrust trajectory analyses to bound spacecraft design parameters for a large class of NEO missions, then detailed array performance models are used to examine the array output voltage and current over a bounded mission set. Operational relationships between the power and electric propulsion systems are discussed, and it is shown that both the SPT-100 and BPT-4000 PPUs can perform missions over a solar range of 0.7 AU to 1.5 AU – encompassing NEOs, Venus, and Mars – within their operable input voltage ranges. A number of design trades to control the array voltage are available, including cell string layout, array offpointing during mission operations, and power draw by the Hall thruster system.

Nomenclature

| | |
|-------------|--|
| A_{cell} | = solar cell area, m ² |
| f_{cm} | = current degradation factor for cell mismatches in layup |
| f_{vm} | = voltage degradation factor for cell mismatches in layup |
| f_{rad} | = degradation factor for environmental radiation |
| f_{other} | = degradation factor for ultraviolet light and micrometeoroids |
| I_{mp} | = cell current at the maximum power point, after applying degradation and environmental factors, A |
| I_o | = dark saturation current, A |
| I_{sc} | = cell short circuit current after applying degradation and environmental factors, A |
| j_{sco} | = cell short circuit current density at standard conditions, A/m ² |
| j_{mpo} | = cell current density at the maximum power point, at standard conditions, A/m ² |

^{*} Senior Engineer, Electric Propulsion Group, Senior Member AIAA.

[†] Project Systems Engineer, Mission Systems Concepts, Senior Member AIAA.

[‡] Mission Design Engineer, Outer Planet Mission Analysis Group.

[§] Engineer, Power Systems Engineering Branch.

^{**} Senior Engineer, Space Propulsion Branch, Senior Member AIAA. Now at Space Systems/Loral, Palo Alto, CA, 94303.

^{††} Aerospace Engineer, Space Propulsion Branch, Member AIAA.

| | | |
|---------------------|---|--|
| N_s | = | number of solar cells in series for each string |
| N_p | = | number of parallel strings of solar cells |
| P_{bus} | = | power required by the spacecraft bus, W |
| P_{EP} | = | power required by the electric propulsion subsystem, W |
| P_o | = | solar irradiance at 1 AU, 1375 W/m ² |
| R | = | spacecraft distance from the sun, Astronomical Units (AU) |
| T | = | cell operating temperature, °C |
| V_{oco} | = | cell open circuit voltage at standard conditions, A |
| V_{oc} | = | cell open circuit voltage after applying degradation and environmental factors, A |
| V_{mpo} | = | cell voltage at the maximum power point, at standard conditions, A |
| V_{mp} | = | cell voltage at the maximum power point, after applying degradation and environmental factors, A |
| ΔV_{diode} | = | voltage drop across array blocking diodes, V |
| ΔV_{wiring} | = | voltage drop in solar array wiring, V |
| α_f | = | absorptivity of solar cell front side |
| β_{isc} | = | temperature coefficient for cell short-circuit current, 1/°C |
| β_{imp} | = | temperature coefficient for cell max-power current, 1/°C |
| β_{Vmp} | = | temperature coefficient for cell max-power voltage, 1/°C |
| β_{Voc} | = | temperature coefficient for cell open-circuit voltage, 1/°C |
| ϵ_f | = | emissivity of solar cell front side |
| ϵ_b | = | emissivity of solar array back side |
| σ | = | Stefan-Boltzmann constant, 5.67×10 ⁻⁸ W/m ² -K ⁴ |
| θ | = | solar array offpointing angle, deg |
| $,array$ | = | solar array parameter for summed series and parallel arrangement of cells |

I. Introduction

Near-Earth Objects (NEOs) are a large class of primitive bodies in the inner solar system that are scientifically interesting for their potential to yield insight into the birth and formation of our solar system; they are often referred to as the leftover debris of the planet formation process. NEOs, which include both comets and asteroids, are specifically those primitive bodies that have settled into orbits that allow them to enter the neighborhood of the Earth (i.e. a perihelion less than 1.3 AU). Several thousand NEOs have been discovered to date (nearly 8,000 as of May 2011¹) and with frequent new findings the total amount is growing rapidly. More than 1,200 of these have been classified as potentially hazardous objects for Earth. There is large diversity in NEOs, and recent investigations suggest new scientific findings are possible with continued exploration.

Recently, the Augustine Commission released a report on the future of manned space exploration and suggested that a “Flexible Path” including manned exploration of NEOs would be a viable and important pathway to Mars. A preliminary study of Flexible Path options concluded that NEOs “have the lowest ‘price of entry’ of any human exploration missions to natural bodies” because of relatively short trip times, lack of large gravity wells, and less required technology development.² Prior to manned exploration, however, robotic precursor exploration would be necessary for determination of target characteristics (e.g. size, morphology, rotation rate), potential resources (water ice, minerals), and potential hazards (radiation, dust), among other things. Precursor spacecraft could even be used during a manned mission as navigation aids, object monitors, and science relays.²

Candidate target surveys for manned missions have found only extremely limited options for exploration with chemically-propelled spacecraft using reasonable assumptions, for example: 9 possibilities out of a field of 1200 NEOs,³ and 58 possibilities out of the several thousand NEOs in the JPL small body database.⁴ These specific results are, of course, a function of the study assumptions. The use of Solar Electric Propulsion (SEP) in conjunction with chemical propulsion in the mission architecture vastly expands the range of accessible targets, allowing manned visits to roughly an order-of-magnitude more NEOs of any given size within any given year.⁵ SEP provides the capability for exploration of more meaningful bodies without the launch window constraints of chemical-only propulsion.

Exploration with unmanned spacecraft significantly expands the base of available targets. A recent study performed in support of the Planetary Science Decadal Survey searched for opportunities among 7,030 asteroids for chemically-propelled missions and identified 624 bodies for rendezvous missions and 345 for Earth-return

missions.⁶ Similar to the manned mission results, the use of SEP vastly expands the set of possible destinations and sends more mass resulting in more and better science. Preliminary trajectory analysis performed as a part of this study suggests that nearly any interesting NEO can be reached within a few years with complete flexibility in launch date. SEP also enables new types of trajectories that are not feasible with chemical propulsion, including missions to multiple targets.

Although exploration of NEOs is necessary as a precursor to manned exploration, there is substantial value in scientific exploration alone. The number and diversity of NEOs suggests that visits to multiple different classes of bodies will return richer scientific and engineering knowledge than visits to one or two easily-reachable targets. Hence, a small inexpensive spacecraft design, one in which multiple spacecraft can be launched on a single dedicated launch vehicle or as a secondary payload, could be an ideal explorer. Such a spacecraft would employ SEP to simultaneously keep the mass low and also open up a broad range of targets. The use of hardware that has already flown, including that from commercial product lines, would keep development and recurring costs down. Innovative SEP trajectory design can be used to reach nearly any NEO in a reasonable time and return significant science data.

Hall thrusters have been shown to provide better mission performance than ion thrusters for near-Earth asteroid sample return missions,⁷ and preliminary work in the present study has shown advantages for Hall thrusters in a small-spacecraft rendezvous application. Commercially-available options include the SPT-100 and the BPT-4000 electric propulsion systems. The SPT-100 has flown on more than twenty Russian and Western communications satellites^{8,9} and the BPT-4000 just recently launched on its first spacecraft. Although both systems were developed for geostationary spacecraft, they can be easily used for NASA deep-space missions.⁷ The SPT-100 thruster is produced by Fakel in Russia and the PPU is produced by Space Systems/Loral. Both the BPT-4000 and its PPU are produced by Aerojet.

One issue with the use of these commercially-developed Hall thruster systems is that the PPUs were designed to operate off of regulated spacecraft power busses, as this bus architecture is advantageous for geostationary communications satellites. The SPT-100 PPU is designed to run off of a 100-V regulated bus,⁹ while the BPT-4000 PPU off of a 70-V regulated bus.¹⁰ NASA deep-space missions, however, typically use unregulated busses where the bus voltage can vary over a wide range. For example, the Dawn mission which employs the NSTAR ion thruster uses an unregulated bus power architecture, designed to accommodate a variable voltage range due to solar distance.^{11, 12} The Dawn PPU was designed and qualified to work over a bus voltage range of 80 to 140 V.¹³ Typically the use of a bus voltage regulator does not trade well for these types of missions.

The mass penalty and costs associated with developing a new bus voltage regulator are in opposition to the goal of a small, inexpensive NEO explorer spacecraft. Similarly, the development costs associated with modifying a commercial PPU to accept a wider range of input voltages are not desirable. Therefore, we undertake in this study an integrated design of the SEP and power subsystems that can enable use of commercially-available hardware without hardware modifications (or as little modification as possible) in a small, inexpensive, heritage-based NEO explorer spacecraft. This effort is generally applicable to other SEP missions in the range of orbits between Venus and Mars.

II. Study Framework and Models

A number of different analyses were required to perform the integrated power and SEP system design. Beginning with an initial set of notional spacecraft requirements, target bodies, and a simple spacecraft power model, trajectory analysis was performed using thruster performance models. With these results, a detailed solar array performance model was used to calculate the available spacecraft power and bus voltage. The models and analyses methods are described in the following sections.

A. Basic Spacecraft Requirements

Requirements for SEP systems do not flow down in quite the same way as do requirements for chemical propulsion systems because of the integrated nature of the design process. The mission designer will start with some idea of spacecraft mass, desired mission timeline, and available electrical power, and investigate different EP

Table 1. Notional Spacecraft Requirements Driving SEP System Selection.

| Parameter | Value |
|-----------------------------|---------------|
| Spacecraft Dry Mass | 150 – 300 kg |
| Spacecraft Electrical Power | 1.5 – 3.0 kW |
| Flight time to Trajectory | ~ 3 years max |
| SEP Engine Throughput | ~ 40 – 120 kg |

system options while trading the mission performance parameters to produce a set of solutions. A rough set of requirements used to guide the SEP system selection process for this study is given in Table 1. Preliminary analyses showed that the flight-proven SPT-100 and BPT-4000 systems provided the best combination of performance along with near-term availability and low cost risk for the NEO missions of interest.

Although chiefly used for primary propulsion, an additional requirement levied on the SEP system was that it be available for limited-duration thrusting during coast phases for events such as course corrections or momentum wheel unloads. Hence, the system was required to be able to operate at any point in the trajectory, not just for deterministic thrusting.

B. PPU Performance

The PPUs for the SPT-100 and BPT-4000 systems were designed for operation on commercial spacecraft with regulated voltage buses, as opposed to the unregulated bus architecture typically employed on NASA robotic spacecraft. The SPT-100 PPU has been qualified to operate over an input voltage range of 95 V to 105 V (nominally 100 V), and the BPT-4000 PPU has been qualified for an input voltage range of 68 V to 74 V (nominally 70 V). A major focus of this study was the integrated design of the power system architecture with the EP system to accommodate variable-voltage output of the solar array while maintaining EP system performance.

Although the SPT-100 PPU qualification input voltage range is 95 V to 105 V, the unit is able to meet nearly all of its performance requirements within a reasonable deviation from this range.¹⁴ All supply outputs are functional and have been demonstrated by analysis to meet their performance requirements over an input voltage range of at least 80 V to 120 V, with the exception of the discharge supply which meets its performance requirements over the range of 93 V to 120 V. At input voltages less than 93 V, the discharge voltage output to the thruster which is nominally 300 V drops by 3 V per 1 V input voltage drop (i.e. at 92 V input voltage the discharge output is 297 V, at 90 V input voltage the discharge output is 291 V). Circuit modeling has been performed to demonstrate operation of all converters over the range of 80 V to 120 V. Unit testing outside of the 95 V to 105 V range has not been performed. There are no issues with component performance or usage at input voltages as low as 80 V. At input voltages greater than 105 V the input capacitors on the all converters do slightly exceed the SS/L derating requirement. Operation at higher input voltages, however, is associated with larger spacecraft solar ranges and hence lower-power EP system operation. Hence, parts derating issues at higher voltages should be mitigated by operation at lower power (i.e. lower thermal dissipation). A review of the circuits by mission assurance in this case would be warranted. PPU-100 efficiency is 94% at the nominal thruster operating condition of 1350 W (300 V and 4.5 A). A quadratic dependence of efficiency on power was assumed here, with an assumed efficiency of 87% at a thruster power of 600 W (300 V and 2.0 A).

The BPT-4000 is also operable outside of its qualification range of 68 V to 74 V, but significantly expanding the range would require hardware changes.¹⁵ Nominally, internal resistor dividers limit operation of the unit to an input voltage range of 65 V to 80 V, but a simple resistor modification can expand the range to at least 55 V to 85 V. The unit will meet all performance requirements over this broad range with the exception of the output voltage range. The BPT-4000 PPU discharge voltage output is commandable from 150 V to 400 V in 50 V increments. At an input voltage of 60 V or greater the PPU can provide a 400 V discharge voltage, but it can only provide 350 V at input voltages from 55 to 60 V. Unit electrical efficiency, which is greater than 92% at nominal conditions, will be no less than 87% worst-case over the 55 V to 85 V input range. At voltages higher than the nominal range, the part stress and derating margins may not be met at full power. However, as operation would be limited to less than 1.5 kW at these voltages and the PPU has been designed for operation at output powers up to 4.5 kW, these issues should be significantly mitigated by the reduced power levels. Circuit review by mission assurance would be necessary.

A summary of the input voltage ranges for both PPUs is shown in Table 2. An alternative PPU implementation path would be a modification of either unit to permit a wider range of input voltages. Preliminary engineering work is already underway on BPT-4000 PPU modification for voltage ranges of interest to NASA science missions.¹⁶ With the emphasis on low cost and the use of already-

Table 2. PPU Input Voltage Ranges.

| Parameter | SPT-100 PPU | BPT-4000 PPU |
|--|-------------|--------------|
| Nominal Input Voltage | 100 V | 70 V |
| Qualified Input Voltage Range | 95 – 105 V | 68 – 74 V |
| Known Operable Input Voltage Range (PPU can operate within at least this range and possibly greater) | 80 – 120 V | 55 – 85 V |

flown technology (i.e. limited or no technology development), use of the heritage PPU is still preferred. It is available, however, and a preliminary investigation of the schedule shows that flight units could be ready by Q4 2013. Additional cost and risk would be incurred with this development. Modification of the SPT-100 PPU is a much less attractive option, largely because of the limited application of the unit for other NASA science missions.

C. Thruster Performance Models

Although used typically at only a single operating point for commercial satellites, the SPT-100 and its PPU are capable of operating over a broad range of powers. The PPU provides a single-point discharge voltage of 300 V but variable discharge current. Thruster performance data taken from work by Brophy et al.¹⁷ and Sankovic et al.¹⁸ were used to develop a thruster performance model for this study. Only those data acquired at discharge voltages of 300 V were used, and all of the thrust data were conservatively de-rated by 6% to account for the normal performance variations throughout life for this engine.^{19, 20} Additionally, the latter study did not employ the standard SPT-100 xenon flow controller (XFC), so only data acquired with cathode flow fractions of 7-9% are shown here (the nominal cathode flow fraction provided by the flight XFC is approximately 8%).⁹ Two additional data points at low powers are included here where additional magnet current was applied to optimize performance.²¹ The de-rated thrust data are shown in Fig. 1 as a function of PPU input power, along with the thrust model implemented in the MALTO trajectory analysis. A similar expression was developed for mass flow rate based on the experimental data.

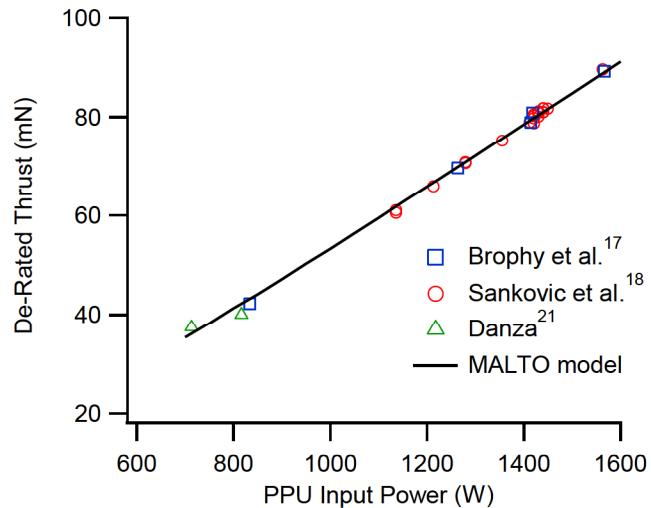


Fig. 1. SPT-100 Performance at 300 V Discharge.

The BPT-4000 system is capable of operating over a range of discharge currents as well as at a number of different discharge voltages, with a power range of a few hundred Watts to almost 5 kW. For this study, the maximum thruster power is limited by the assumed solar array power available. The engine performance curves used for trajectory analysis were taken from published “high-thrust” BPT-4000 performance models.²²

D. Trajectory Analysis

A large number of different asteroids were identified as attractive targets for robotic exploration, and analyses were performed for multiple combinations of targets, spacecraft masses, and spacecraft powers. Trajectory analysis was performed using JPL’s MALTO low-thrust optimization tool.²³ Inputs for the analysis included the target orbits, the engine performance model from Section C, and a power model based on a preliminary solar array design. The trajectory optimizer selects the engine power and burn duration for each time step in an analysis interval. For the NEO trajectories investigated, the engine is nearly always operated at the maximum possible power. Engine power is reduced accordingly as the array power diminishes at larger solar ranges.

One set of analyses for six different target bodies will be discussed here. Assumptions for the analyses were: a 300 kg mass was delivered for a ninety-day rendezvous with the target, the solar array was sized for 2.2 kW of electrical power at 1 AU with end-of-mission level degradations, the spacecraft bus load was a constant 250 W, and the SPT-100 system was employed with a thruster power range of 0.6 kW to 1.5 kW. Any excess array power not used by the bus or SEP system was assumed to be shunted off. The engine was also required to be available for non-deterministic thrusting during the rendezvous period and was subject to a throughput limitation of 120 kg (the demonstrated throughput by test is ~180 kg⁹). Thruster operation during each of the spacecraft trajectories is shown graphically in Fig. 2. The 0.7 to 1.5 AU operational range is important because, along with the power system design, it defines the array voltage available for PPU input. Most thruster operation occurs between 0.7 AU and 1.2 AU. Some operation at larger ranges is required for 1991 JW and 1989 UQ. If it were not a requirement for the EP system to be available for thrusting at any point in the trajectory, those trajectories could be further refined to force coasting at ranges greater than 1.2 AU. This would have the added benefit of reducing the input voltage range for the PPU.

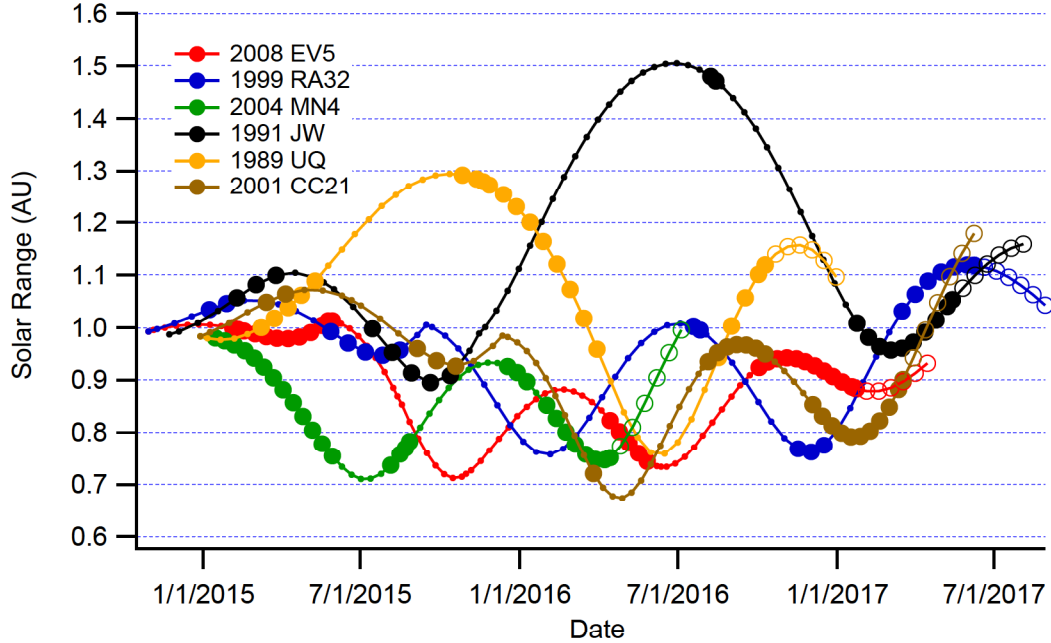


Fig. 2. Typical Spacecraft Trajectory Set for Missions Using the SPT-100. The spacecraft is either thrusting (solid circles) or coasting (small tickmarks) prior to rendezvous with the target body (open circles). Trajectories utilizing the BPT-4000 span a similar set of solar ranges.

Several different trajectories were calculated for the BPT-4000 system using similar sets of assumptions. Because the targets are in the same orbits regardless of the type of EP system, the span of solar ranges in the trajectories is not significantly different. Hence, to facilitate the presentation of the results here, both the SPT-100 and BPT-4000 PPUs were evaluated against the same solar range of 0.7 to 1.5 AU.

E. Solar Array Performance Model

Solar irradiance and cell temperature have a large effect on solar array performance and change throughout the course of the planned trajectories and with spacecraft operational states. This necessitates an array performance model that can predict the solar array output voltage (i.e. the PPU input voltage, also known as the bus voltage) over the course of the mission duration. The model that is developed here combines a simple array thermal model with a cell performance model that accounts for degradation effects, temperature effects, distance from the sun, and array orientation.

An ATK UltraFlex solar array with Emcore ZTJ triple-junction GaInP₂/GaInAs/Ge cells was selected for this study. The UltraFlex array design successfully flew on the Mars Phoenix mission. While this type of array design favors certain multiples of string counts for the best combination of cost, mass, and performance, string counts considered here are allowed to take any value to demonstrate the combined power and propulsion system performance and design. The results presented here are independent of array design.

Relevant performance data for the ZTJ cells are shown in Table 3 under simulated illumination at 1 AU and 28 °C. The bare cell data (j_{sco} , j_{mpo} , V_{oco} , V_{mpo}) were taken from Fig. 2 of Cho et al.²⁴ The temperature coefficient data shown in Table 3 are the values from Table 9 of Stan et al.²⁵ for the zero fluence case, normalized using the bare cell data. A cell size of 17.59 cm² (A_{cell}) was assumed.

Cell performance was adjusted for degradation, distance from the sun, array orientation, and operational temperature using standard cell modeling techniques applied to this design,²⁶ resulting in the expressions given in Eqs. 1-4:

Table 3. Emcore ZTJ Solar Cell Properties.^{24, 25}

| Cell Parameter | Value |
|----------------|------------------------|
| j_{sco} | 173.5 A/m ² |
| j_{mpo} | 165.9 A/m ² |
| V_{oco} | 2.731 V |
| V_{mpo} | 2.410 V |
| β_{IsC} | 0.000674 / °C |
| β_{mp} | 0.000549 / °C |
| β_{Voc} | -0.0023 / °C |
| β_{Vmp} | -0.0028 / °C |

$$I_{sc} = (j_{sco}A_{cell})f_{cm}f_{rad}f_{other} \frac{\cos\theta}{R^2} \{1 + \beta_{I_{sc}}(T - 28)\} \quad (1)$$

$$I_{mp} = (j_{mpo}A_{cell})f_{cm}f_{rad}f_{other} \frac{\cos\theta}{R^2} \{1 + \beta_{I_{mp}}(T - 28)\} \quad (2)$$

$$V_{oc} = V_{oco}f_{vm}f_{rad} \frac{\ln(\frac{I_{sc}}{I_o})}{\ln(\frac{j_{sco}A_{cell}}{I_o})} \{1 + \beta_{V_{oc}}(T - 28)\} \quad (3)$$

$$V_{mp} = V_{mpo}f_{vm}f_{rad} \frac{\ln(\frac{I_{sc}}{I_o})}{\ln(\frac{j_{sco}A_{cell}}{I_o})} \{1 + \beta_{V_{mp}}(T - 28)\} \quad (4)$$

where I_{sc} is the cell short circuit current, V_{oc} is the open circuit voltage, and I_{mp} and V_{mp} are the current and voltage at the maximum power point, respectively. The cell current decreases with increasing solar range (R), decreases as the solar arrays are tilted away from the sun (θ , called “offpointing”), and slightly increases with cell temperature (T). Cell voltage decreases with increasing cell temperature and exhibits a smaller dependence on intensity through the natural logarithm terms.

Array degradation due to radiation effects was calculated for a typical trajectory and flight duration using a standard radiation treatment.²⁷ A power degradation factor of 0.92 for radiation was applied to all cases, in equal parts to cell current and voltage (f_{rad}). Additional degradation factors were applied to the individual current and voltage terms to account for losses due to ultraviolet effects, micrometeoroid and orbital debris (f_{other}), and mismatch and fabrication losses (f_{cm} , f_{vm}). The array modeling assumptions are summarized in Table 4. Each solar array is built from groups of cells connected in series (N_s) and strung in parallel (N_p) in order to achieve the desired array voltage and output power as shown in Eqs. 5-8. It was assumed that each parallel string contained a blocking diode and there was some fixed voltage loss in the wiring. Losses of 0.6 V and 1.5 V, respectively, were used here.

Table 4. Solar Array Model Assumptions.

| Parameter | Value |
|--------------|---------------------------------------|
| f_{cm} | 0.98 |
| f_{vm} | 0.99 |
| f_{rad} | 0.96 |
| f_{other} | 0.98 |
| I_o | 5×10^{-12} A |
| A_{cell} | 17.59×10^{-4} m ² |
| α_f | 0.92 |
| ϵ_f | 0.90 |
| ϵ_b | 0.60 |

$$I_{sc,array} = I_{sc}N_p \quad (5)$$

$$I_{mp,array} = I_{mp}N_p \quad (6)$$

$$V_{oc,array} = V_{oc}N_s \quad (7)$$

$$V_{mp,array} = V_{mp}N_s + \Delta V_{diode} + \Delta V_{wiring} \quad (8)$$

A simple one-dimensional, single-node thermal model was used to calculate the cell temperature by balancing incident radiation from the sun with cell thermal radiation and electrical power drawn by the spacecraft. This power balance is shown in Eq. 9, where it was assumed that the array was entirely covered with solar cells and was thermally isolated from the spacecraft. Optical properties obtained for the Emcore ATJ solar cells were assumed to be similar to the ZTJ cells and were used for this analysis (absorptance of 0.92 and emissivity of 0.90).²⁸ The net emissivity of the back side of the array was assumed to be 0.60. A solar irradiance at 1 AU of 1375 W/m² was used. Based on limited application of similar models to orbital test cases, an uncertainty of ± 10 °C is expected in the calculated temperatures.

$$\alpha_f P_o \frac{\cos\theta}{R^2} (N_s N_p A_{cell}) = (\epsilon_f + \epsilon_b) \sigma (N_s N_p A_{cell}) (T + 273.15)^4 + P_{bus} + P_{EP} \quad (9)$$

Given the distance from the sun, the array offpointing angle, the array stringing (N_p , N_s), and the spacecraft operational state (P_{bus} , P_{EP}) the cell temperature can be calculated. With the temperature, the four array performance parameters ($I_{sc,array}$, $I_{mp,array}$, $V_{oc,array}$, $V_{mp,array}$) may be determined. Finally, these factors can be used to define the array performance curve, i.e. the current-voltage curve. In this study the formulation of Rauschenbach²⁶ was used to calculate that curve. In addition to the temperature uncertainty, sources of uncertainty for array modeling include for example the solar cell performance factors (Table 3), degradation factors and thermal properties (Table 4), and the actual bus power draw (it will not be a constant 250 W). In lieu of a complete uncertainty analysis, the effect of temperature uncertainty on the bus voltage is given in the Results sections as an example of uncertainty magnitudes.

III. Results

The nominal design point for the solar array in this study was to provide 2.2 kW of electrical power at 1.0 AU at end-of-mission. The spacecraft is expected to operate at solar ranges from approximately 0.7 to 1.5 AU, and it can tolerate lower power levels at distances greater than 1 AU. The solar array output voltage is limited to a range defined by the operation of the SEP system PPU. For the SPT-100 system, the nominal PPU input voltage is 100 V and the array output voltage is limited to a range of 80 V to 120 V, preferably with a minimum of 90 V. For the BPT-4000 system, the nominal PPU input voltage is 70 V and the array output voltage is limited to a range of 55 V to 85 V. For both systems it is advantageous but a requirement to limit the maximum array voltage to the upper limit of the qualification range because of potential parts deratings issues. Because both systems are under consideration, there must be two separate array electrical designs.

All analysis results presented here assume an array design which produces 2.2 kW of electrical power at 1 AU with all array degradations for the mission duration (e.g. radiation and micrometeoroid) applied at the beginning of the mission to simplify the analysis, except where noted. The spacecraft bus power draw, i.e. the power used by the spacecraft for everything but electric propulsion, was assumed to be a constant 250 W. At sufficiently large solar ranges the spacecraft cannot provide full power to the EP system; in these cases the maximum power that could be provided was calculated based on the available power. There was no power margin assumed for the EP system and the spacecraft was allowed to operate at the array peak power point. This would not be the case for actual mission operations, but as will be seen it presents a conservative case for the total bus voltage range experienced during a mission.

A. Operational Relationships

To understand the system relationships and design drivers, first consider a solar array designed to produce 2.2 kW of power at 1 AU with no power draw for EP. Using the array performance models to produce a design with a nominal 100 V bus voltage at 1 AU yields 94 strings of 44 cells each. The bus voltage produced by the array during the mission depends largely on the cell temperature through three parameters: the solar range (R), the array offpointing angle (θ), and the power used by the EP system (P_{EP}).

The calculated cell temperature and bus voltage for the solar ranges of interest are shown in Fig. 3. A wide range of cell temperatures is observed, and the corresponding bus voltage range is about 30 V, from 85 V to 115 V. The SPT-100 PPU is capable of operating over this wide range, but there are performance losses at voltages less than 93 V and there may be parts derating issues at voltages

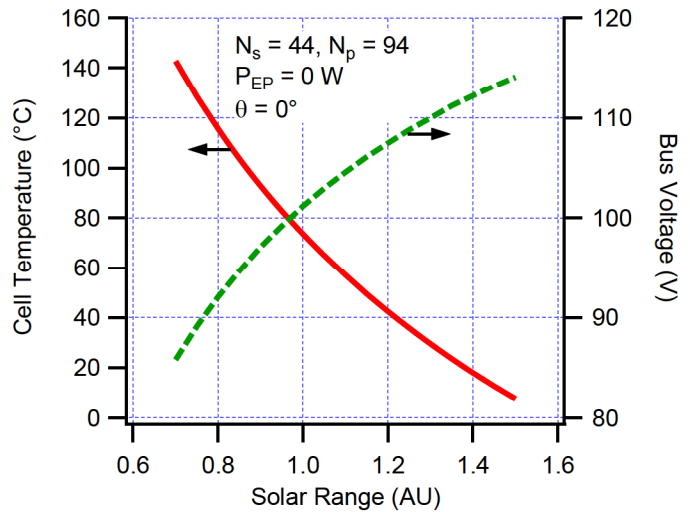


Fig. 3. Effect of Solar Range on Temperature and Voltage.

greater than 105 V. It would be ideal to design the system to keep the bus voltage between 93 V and 105 V, a range about half of that shown in Fig. 3. A bus voltage of only 90 V may still be acceptable as the performance losses at this input would be very small.

The cell temperature can be decreased by offpointing the arrays to reduce the incident solar energy as seen in Eq. 9. This is most effective nearest the sun where the cell temperature is highest and the excess power produced by the arrays may not be useful. Shown in Fig. 4 are the calculated cell temperatures and bus voltages for a range of array offpointing angles at the closest point to the Sun in the trajectory. At 0.7 AU the cell temperature can be reduced by over 60 °C by offpointing the arrays by 60°. This has the effect of increasing the bus voltage by 15 V, which would cut in half the bus voltage range experienced over 0.7 to 1.5 AU. Array offpointing thus simultaneously provides two advantages to the system – reduction of cell temperature and reduction of the bus voltage range that would be seen by the EP system PPU. Large offpointing angles have the potential to lead to spacecraft operational difficulties and risks to the supply of power, although those risks need to be evaluated on a mission-specific basis.

The final parameter with an effect on the bus voltage is the power draw by the EP system, which was limited to between 700 and 1575 W for the SPT-100. This dependence is shown in Fig. 5 for four solar ranges. At 1 AU and closer to the sun the arrays produce sufficient power to operate the EP system at full power. Here, the bus voltage changes by only about 1 V over the entire range of EP system powers, and the difference in bus voltage when the system is off is only about an additional 1 V. At ranges larger than 1 AU, however, the EP system power is limited by the maximum array power and the bus voltage dependence on EP power is much greater. Here, the bus voltage changes by about 5 V over the range of EP powers, and is 0.5 to 1.5 V higher when the EP system is off than when it is drawing 700 W. At all solar ranges, the effect of EP system power draw on bus voltage is much less than the effect of temperature change due to changing distance from the Sun.

The array power balance in Eq. 9 shows that for fixed solar range and offpointing angle, cell temperature decreases as the EP system power is increased. Recall that solar cell voltage increases with decreasing temperature, yet Fig. 5 shows the net effect of increasing EP power draw is to decrease the bus voltage. These competing effects are illustrated in Fig. 6 for a spacecraft at 1.2 AU and no array offpointing. The cooling effect is observed by the shifting of the array power curve to larger voltages as EP power draw is increased. Simultaneously, as the load power is increased the system operating point moves up the power-voltage curve toward the maximum power point. The net effect is that the bus voltage slightly decreases with increasing EP power draw at lower powers, and as the peak power point is reached the array curve flattens out and small changes in power draw cause larger bus voltage changes. This is the cause of the steeper changes in bus voltage visible in the 1.2 AU and 1.5 AU curves of Fig. 5.

During mission operations, the only real control over the bus voltage is found through the array offpointing angle, which is useful only at solar ranges where the load power required is less than the power produced by the array. The solar range and the EP power draw are fixed by the trajectory design. It may be possible in some

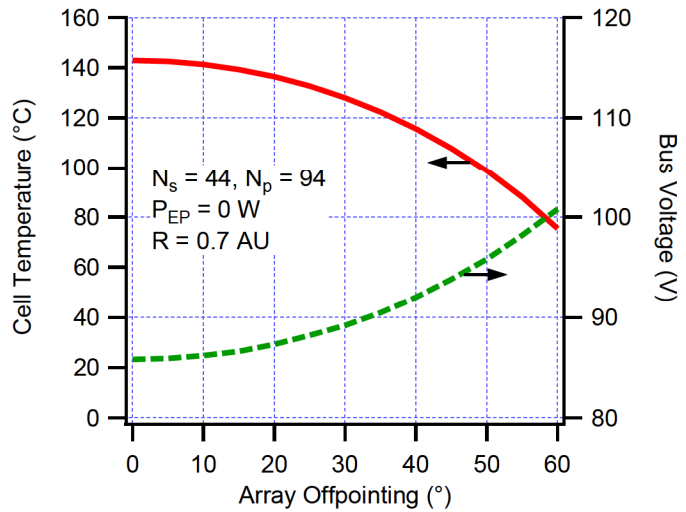


Fig. 4. Effect of Offpointing on Temperature and Voltage.

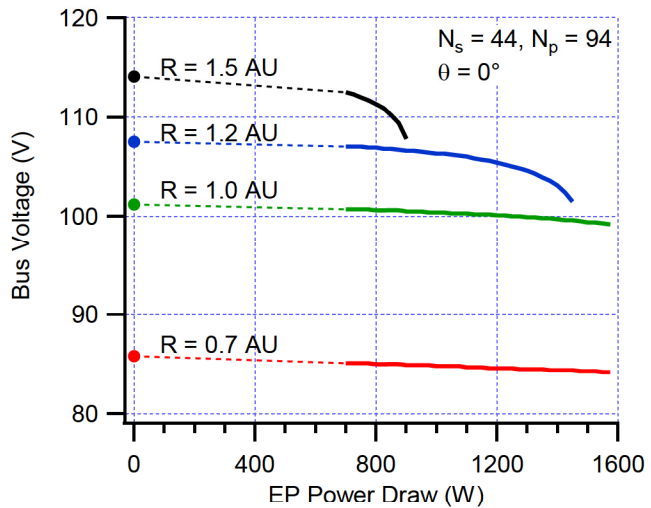


Fig. 5. Effect of EP Power Draw on Bus Voltage.

instances to adjust the EP power draw through trajectory changes, but as has been shown this has only a small effect on the bus voltage.

Finally, recall that the simple thermal model employed here has an estimated uncertainty of ± 10 °C. The uncertainty in bus voltage due to the temperature uncertainty was calculated by substituting 10 °C higher or lower temperatures than those calculated using Eq. 9 into the array performance equations. It was found that this uncertainty depends slightly on the array design. For the design and range shown in Fig. 3 the calculated bus voltage uncertainty was 2.7 V.

B. Design for 100 V bus

The tools developed in Section II were next applied to the design of a power system architecture for the SPT-100 system. The SPT-100 PPU is qualified for operation from 95 to 105 V, although it can operate over a much wider range of 80 to 120 V. The design goal was to limit the maximum input voltage to 105 V in order to avoid parts derating issues, and to limit the minimum voltage to 90 V where the unit performance is only slightly affected (the discharge voltage will be 291 V in this case instead of the nominal 300 V).

Requirements for this design are that the array produce 2.2 kW of electrical power at 1 AU, with end-of-mission degradation factors applied to the array and the SPT-100 system operating at full power. In order to limit the PPU input voltage to 105 V when operating, the number of cells per string was adjusted until the bus voltage was a maximum of 105 V when the SPT-100 system was operating at the minimum power of 700 W. The number of strings was then adjusted to reach the 1 AU power goal. Under these constraints a design of 96 strings of 41 cells each was reached. The variation in bus voltage is shown in Fig. 7 for all solar ranges and the three bounding EP power levels. Note that the SEP system must accommodate the entire bus voltage range from the EP system startup condition ($P_{EP} = 0$ W) to the max power condition because the PPU must remain in its operating voltage range as the thruster transitions from off to full (or maximum available) power. Note also that some iteration between Eq. 9 and

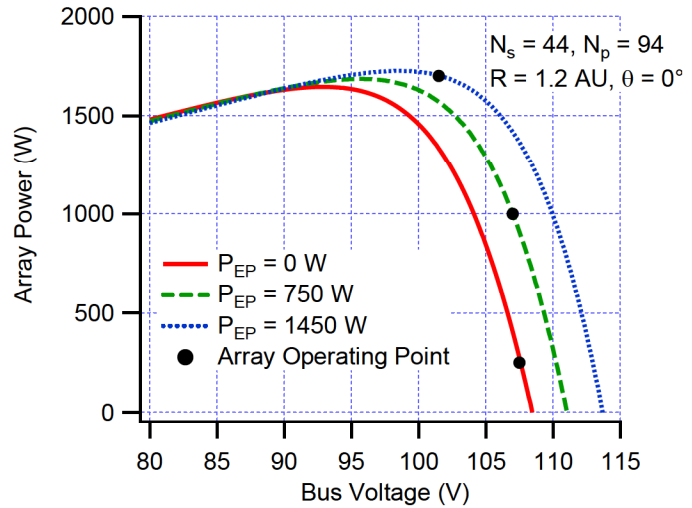


Fig. 6. Effect of EP Power Draw on Array Power Curve.

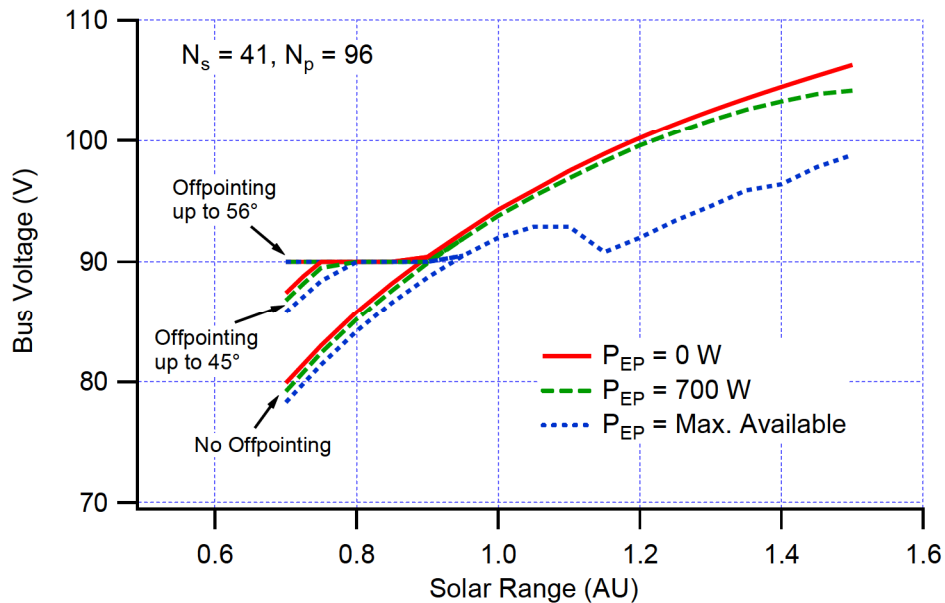


Fig. 7. Bus Voltage Range for SPT-100-based EP System.

Eqs. 1-8 is required in order to match the EP power draw with the array peak power point. Bus voltage uncertainty due to temperature uncertainty was 2.5 V for the data shown in Fig. 7. This configuration produces bus voltages near 80 V at 0.7 AU with no offpointing. To stay within the design goal for bus voltage the array must be offpointed by up to 56°. If offpointing no greater than 45° is allowed, the bus voltage would be 86 V minimum during SPT operation. Nonetheless, it can be seen that bus voltage range can be designed to be well within the operable limits of the SPT-100 PPU of 80 V to 120 V.

The power system configuration detailed in Fig. 7 was designed for maximum bus voltage of 105 V during SPT operation in order to avoid possible parts derating issues at higher voltages. Two items should be noted here. First, when the EP system is off the bus voltage is slightly higher at a value of 106 V. When the PPU is turned on to ignite the thruster its startup sequence will begin at a bus voltage between 105 V and 106 V, and as soon as the discharge ignites the power draw will pull the bus voltage down to 105 V or less. This transitory, low-power operation may or may not be important with respect to parts derating. Second, the standard parts deratings applied for high-current and high-temperature PPU operation may not be applicable at the larger solar ranges where the system is operating at 850 W, or slightly more than half of the maximum system power. These items should be reviewed by a mission assurance team to determine if a wider bus voltage range would be permissible. If higher-voltage operation at larger ranges is preferred over array offpointing at smaller ranges, the array could be re-strung to increase bus voltages at all ranges as shown in Fig. 8. If this is desired, a more detailed design trade would have to be made involving parts derating issues for the PPU at input voltages above 105 V, the system performance at input voltages less than 90 V, and operation of the spacecraft with array offpointing at angles greater than 45°.

While the bus voltage in Fig. 7 shows monotonic behavior for both 0 W and 700 W EP power, the behavior for the maximum EP power draw is more interesting. To examine this in greater detail, array power curves are shown for three ranges in Fig. 9. As the solar range increases the maximum array power decreases (due to lower light intensity) and the voltages shift higher (due to lower cell temperatures). At 1.1 AU the array produces sufficient power for the EP system to operate at full power and there is excess array power beyond what the spacecraft and EP system can use. Further out at 1.15 AU the array no longer can provide full power to the EP system, instead the EP system draws all available power from the array, operating at a reduced 1515 W. Here, the spacecraft operates at the array maximum power point where the bus voltage is flatter, and the combination of the change in array curve shape and EP power draw causes the bus voltage to be less than that at 1.1 AU. Moving out to 1.2 AU the spacecraft still operates at the maximum array power but at lesser EP powers, and the cooler array temperature has caused the bus voltage to increase compared to the 1.0 and 1.15 AU ranges. A spacecraft would likely not be operated at the array peak power point but with some margin against it, thus the results presented here represent a worst case for the bus voltage lower range.

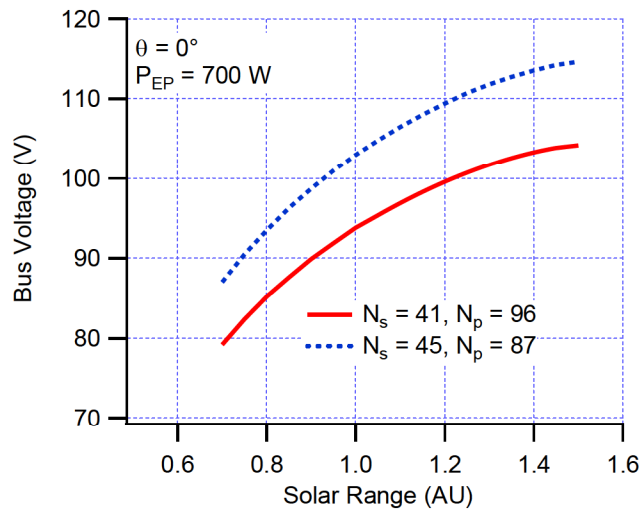


Fig. 8. Effect of Array Stringing on Bus Voltage for 100-V Bus Design.

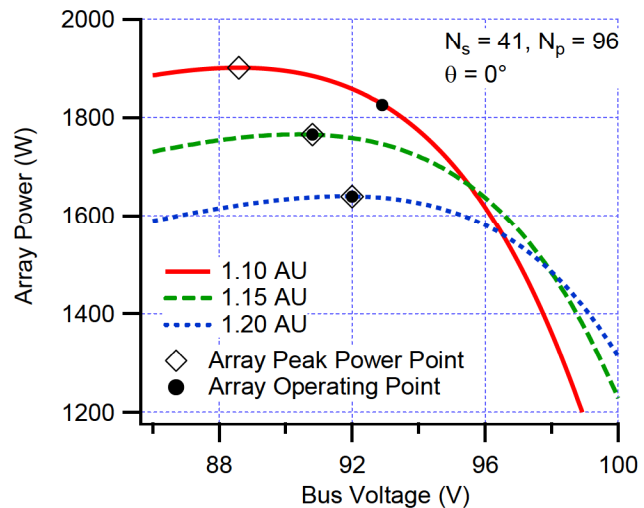


Fig. 9. Detail of Non-Monotonic Bus Voltage Behavior for 100-V Bus Design.

Finally, the bus voltage calculations shown in Fig. 7 show an acceptable range for the SPT-100 PPU for end-of-mission level degradations. In practice, however, the array will perform better at the beginning of the mission and degrade gradually throughout it. The bus voltage range for beginning-of-mission degradation levels was calculated by assuming no degradation due to radiation (i.e. $f_{rad} = 1$) and no degradation due to ultraviolet and micrometeoroid/debris effects (i.e. $f_{other} = 1$). The results are shown in Fig. 10, where it can be seen that beginning-of-mission bus voltages are four to six volts higher across the span of solar ranges. This additional variation with time during a mission will have to be accounted for in the power system design. The SPT-100 PPU is operable at the higher bus voltages (slightly more than 110 V in Fig. 10) but the parts deratings must be investigated.

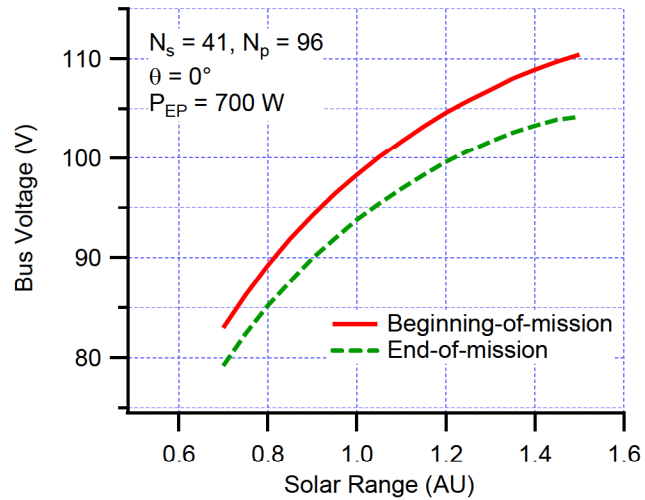


Fig. 10. Effect of Array Degradation on Bus Voltage for 100-V Bus Design.

C. Design for 70 V bus

The electrical design of the previous section was repeated for the power system architecture for the BPT-4000 system. The BPT-4000 PPU is qualified for operation from 68 to 74 V but is operable over a range of at least 55 V to 85 V with a simple resistor modification. The design goal for this system was to limit the maximum input voltage to 74 V in order to avoid parts derating issues, and to limit the minimum voltage to 55 V. It is possible that parts deratings may only be a minor issue at voltages up to 85 V because the PPU is qualified to operate at powers in excess of 4 kW but will only be used to process less power than that.

Requirements for this design are that the array produce 2.2 kW of electrical power at 1 AU, with end-of-mission degradation factors applied to the array and the BPT-4000 system operating at full power. The same solar range of 0.7 to 1.5 AU was evaluated. The number of solar array cells per string was adjusted until the bus voltage was 74 V when the BPT-4000 system was operating at the minimum power of 300 W²² at 1.5 AU. The number of strings was then adjusted to reach the 1 AU power goal of 2200 W with the engine operating at the maximum power possible, 1950 W in this case. Under these constraints a design of 136 strings of 29 cells each was reached.

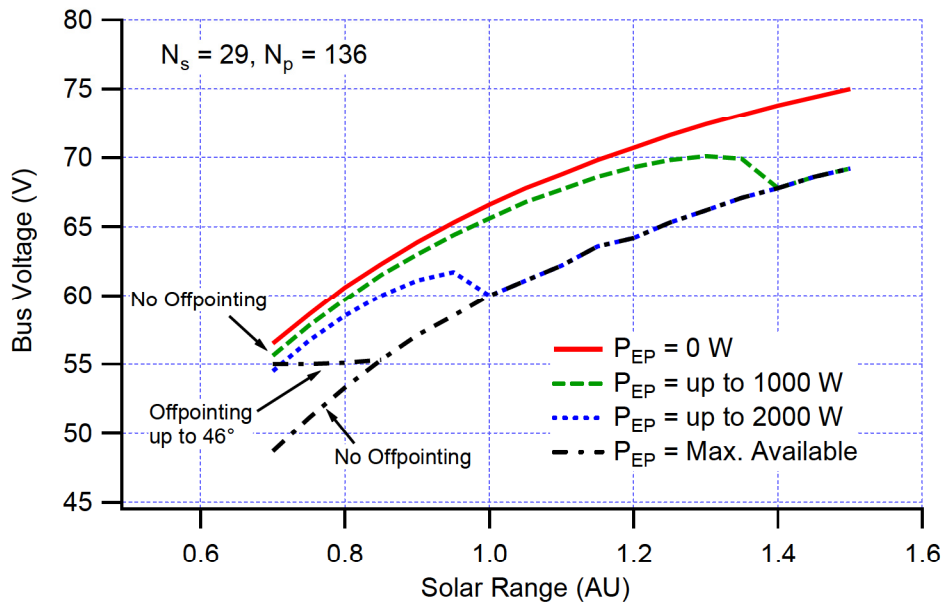


Fig. 11. Bus Voltage Range for BPT-4000-based EP System

The variation in bus voltage is shown in Fig. 11 for all solar ranges and four EP powers. Bus voltage uncertainty due to temperature uncertainty was 1.7 V for these data. The BPT-4000 system has an advantage in that it can use the higher array powers available closer to the Sun. At 1.5 AU the available array power limits BPT system operation to 845 W, while at 0.7 AU and no offpointing the system could operate at 3560 W. The non-monotonic bus voltage behavior at EP powers of 1000 and 2000 W is a result of the system moving along the array power curve, similar to the behavior seen in Fig. 9. Offpointing is not required close to the Sun to keep the bus voltage in the target range, as long as the EP power is limited to less than 1600 W. The bus voltage behavior with increasing EP power at 0.7 AU is similar to that shown in Fig. 6. As EP power is increased the bus voltage slowly decreases until it nears the peak power point at which the bus voltage decreases more rapidly. By offpointing the array up to 46° the EP system can operate at powers up to 2675 W while keeping the bus voltage within the target range.

Note that the range of bus voltages is smaller than for the SPT-100 system. With no EP power the bus voltage varies by 19 V across all solar ranges while for the SPT-100 design the bus voltage range is 26 V. Under these conditions the cell temperatures and cell performance are the same at each range. The net result with the differing string layout is that the ratio of bus voltage change to the nominal bus voltage is about the same for both systems.

Bus voltage range for beginning-of-mission array degradations (i.e. $f_{rad} = f_{other} = 1$) for the minimum EP power level of 300 W is shown in Fig. 12. The upper end of the qualification voltage range for the PPU (74 V) is exceeded at ranges larger than 1.25 AU. The PPU will run at up to 85 V input but some parts deratings may be exceeded at full PPU power. At these ranges, however, the power available for EP is at most 1250 W which is well below the maximum PPU power, thus parts deratings at voltages of up to 78 V may not be an issue. Alternatively, the array could be designed to limit the beginning-of-mission voltage to the qualification limit of 74 V at 1.5 AU. This would cause the bus voltage at 0.7 AU to decrease by a few volts and thus require some array offpointing to hold the bus voltage above the lower limit of 55 V at end-of-mission degradation conditions. This is an example of the type of design trades that are available to the spacecraft design team.

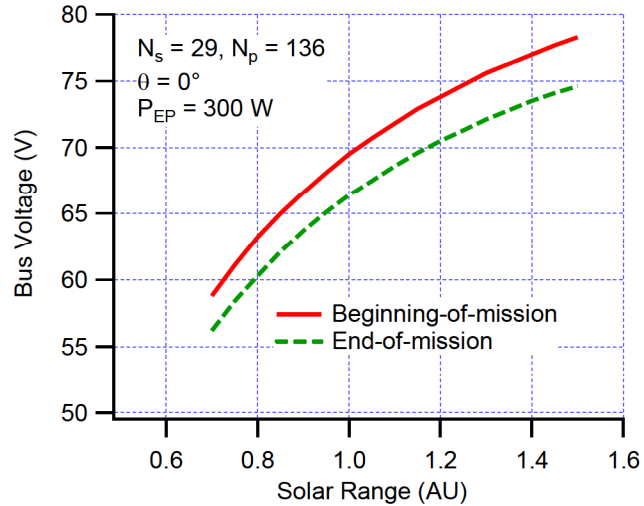


Fig. 12. Effect of Array Degradation on Bus Voltage for 70-V Bus Design.

D. Design Results Summary

A power system design for the SPT-100 PPU that maintains the bus voltage well within the known operable range of 80 V to 120 V is quite feasible, but operation wholly within the qualification range is not feasible. A summary of the results for one stringing design is shown in Fig. 14. The highest bus voltages are expected at the furthest solar range investigated with no in-service array degradation, and the lowest bus voltages are expected at the innermost ranges at end-of-mission degradation levels. Array offpointing is required to maintain the bus voltage within the known operable range, and is also required to keep the voltage above 90 V, which is the point at which the discharge voltage supply output falls below 290 V. As an alternative to array offpointing during the mission, the array stringing could be changed to raise the bus voltage at all operating conditions. This would push the highest voltages into conditions where parts derating issues may be of greater concern. Higher bus voltages can be mitigated by operating the EP system at maximum powers. As can be seen, a number of design possibilities and tradeoffs are available to the spacecraft design team to control the bus voltage.

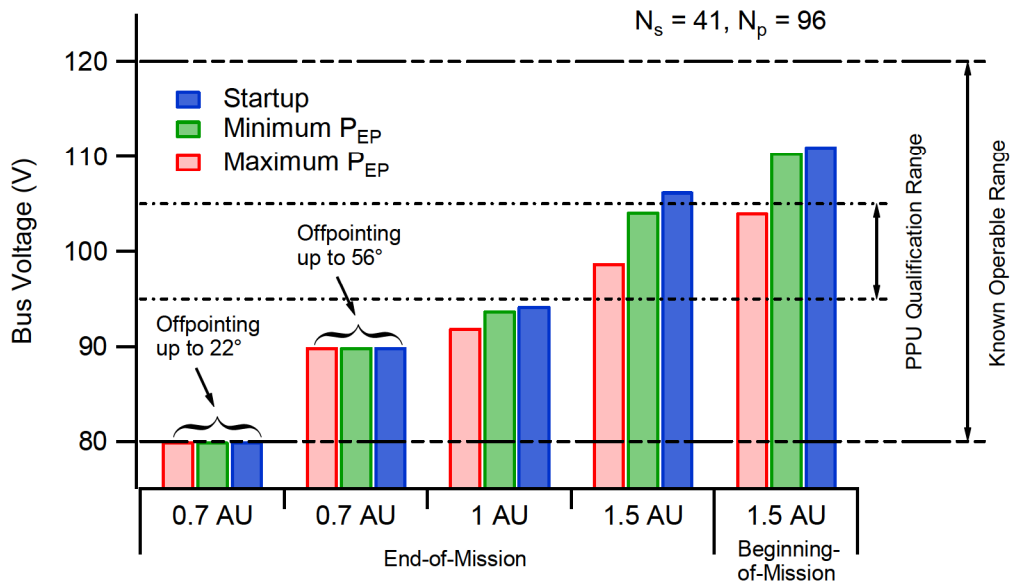


Fig. 14. Bus Voltage Design Summary for SPT-100 System.

A similar depiction of the bus voltage range for the BPT-4000 PPU is shown in Fig. 13. Operation of the PPU within the known operable range, but not within the qualification range, is feasible for this type of mission. For this particular array design, array offpointing is required only at the minimum solar range, and then only for operation at maximum EP power. A bus voltage within the known range could also be maintained by limiting EP power instead of array offpointing. Power system design trades for the BPT-4000 system are somewhat easier than for the SPT-100 system because of the smaller range of bus voltages experienced as a function of solar range, and to some extent the larger range of EP power available to the thruster.

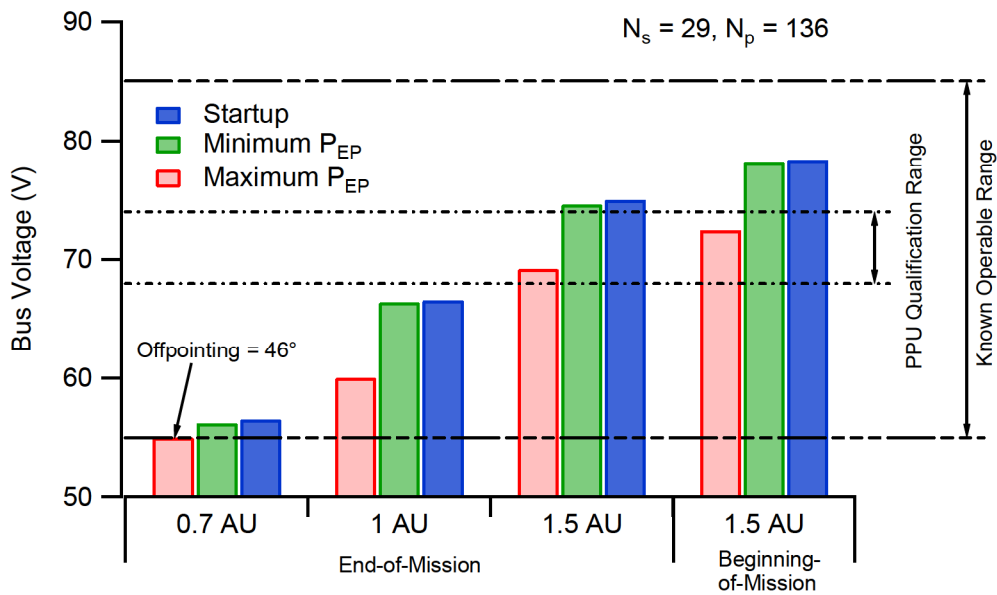


Fig. 13. Bus Voltage Design Summary for BPT-4000 System.

IV. Conclusion

An integrated power and propulsion system design has been developed for two candidate EP systems for near-Earth object exploration, and the design parameters have been investigated. Models for engine performance, solar array performance, and trajectory analysis have been combined to demonstrate the feasibility of using commercial Hall thruster systems for NEO exploration. Trajectories were found to span solar ranges of 0.7 to 1.5 AU and spacecraft bus voltages were calculated across this range for different cases of array offpointing, EP power draw, and array degradation.

For the SPT-100 system, the mission and spacecraft architecture can be designed to maintain the bus voltage well within the known operable range of 80 V to 120 V, but not within the qualification range of 95 V to 105 V. An upper limit of 105 V, equal to the upper bound of the qualification range, would preclude additional analysis of parts deratings and is achievable but would require a tradeoff with either EP system performance or relatively large array offpointing. Alternatively, it is noted that bus voltages between 105 V and 120 V would only be experienced at ranges where the EP system is operating at less than full power, and parts derating issues should be mitigated. If this is the case, performance and offpointing concerns at ranges closer to the Sun would be less of a concern.

For the BPT-4000 system, integrated designs are easily achieved which maintain the bus voltage within the known operable range of 55 V to 85 V, but not within the qualification range of 68 V to 74 V. As for the SPT-100, limiting the bus voltage to 74 V precludes additional analysis of parts deratings, but would require relatively large offpointing at the inner solar system ranges.

Acknowledgments

A portion of the work described in this paper was carried out by the Jet Propulsion Laboratory, California Institute of Technology, under a contract with the National Aeronautics and Space Administration. Funding and guidance for the JPL portion of this work was provided by Mike Sander and John Baker of the Exploration Systems and Technology Office. Special thanks go to Mike Staley and Jim Waranauskas of Space Systems/Loral for information regarding the SPT-100 PPU performance, Tom Danza and Ron Corey of Space Systems/Loral for SPT-100 performance, and to Kristi de Grys and Alex Mathers for BPT-4000 PPU performance.

References

1. Jet Propulsion Laboratory, *Near-Earth Asteroid Discovery Statistics*. [Web Page]; Available from: <http://neo.jpl.nasa.gov/stats> [Cited May, 2011]
2. Sherwood, B., M. Adler, L. Alkalai, L. Burdick, D. Coulter, F. Jordan, F. Naderi, L. Graham, R. Landis, B. Drake, S. Hoffman, J. Grunsfeld, and B.D. Seery, "Flexible-Path Human Exploration," AIAA 2010-8607, AIAA SPACE 2010 Conference, Anaheim, CA, Aug. 30 - Sept. 2, 2010.
3. Landis, R.R., P.A. Abell, D.J. Korsmeyer, T.D. Jones, and D.R. Adamo, "Piloted operations at a near-Earth object (NEO)," *Acta Astronautica*, 2009. **65**(11-12): p. 1689-1697.
4. Adamo, D.R., J.D. Giorgini, P.A. Abell, and R.R. Landis, "Asteroid Destinations Accessible for Human Exploration: A Preliminary Survey in Mid-2009," *Journal of Spacecraft and Rockets*, 2010. **47**(6): p. 994-1002.
5. Landau, D. and N. Strange, "Human Exploration of Near-Earth Asteroids via Solar Electric Propulsion," AAS 11-102, AAS/AIAA Space Flight Mechanics Meeting, New Orleans, LA, Feb. 13-17, 2011.
6. Strange, N., E. Asphaug, K. Grogan, D. Landau, and K. Reh *Near Earth Asteroid Trajectory Opportunities in 2020-2024*. Sept. 2010. http://sites.nationalacademies.org/SSB/SSB_059327. [Cited June 7, 2011]
7. Hofer, R.R., T.M. Randolph, D.Y. Oh, J.S. Snyder, and K.H. de Grys, "Evaluation of a 4.5 kW Commercial Hall Thruster System for NASA Science Missions," AIAA 2006-4469, 42nd Joint Propulsion Conference, Sacramento, CA, July 9-12, 2006.
8. Pidgeon, D.J., R.L. Corey, B. Sauer, and M.L. Day, "Two Years On-Orbit Performance of SPT-100 Electric Propulsion," AIAA 2006-5353, 24th AIAA International Communications Satellite Systems Conference, San Diego, CA, June 11-14, 2006.
9. Corey, R.L., N. Gascon, J.J. Delgado, G. Gaeta, S. Munir, and J. Lin, "Performance and Evolution of Stationary Plasma Thruster Electric Propulsion for Large Communications Satellites," AIAA 2010-8688, 28th AIAA International Communications Satellite Systems Conference, Anaheim, CA, Aug. 30 - Sept. 2, 2010.
10. de Grys, K., B. Welander, J. Dimicco, S. Wenzel, B. Kay, V. Khayms, and J. Paisley, "4.5 kW Hall Thruster System Qualification Status," AIAA 2005-3682, 41st AIAA Joint Propulsion Conference, Nashville, TN, July 10-13, 2005.
11. Fatemi, N.S., S. Sharma, O. Buitrago, J. Crisman, P.R. Sharps, R. Blok, M. Kroon, C. Jalink, R. Harris, P. Stella, and S. Distefano. "Performance of high-efficiency advanced triple-junction solar panels for the LILT Mission Dawn," in *Proceedings of the Photovoltaic Specialists Conference, 2005. Conference Record of the Thirty-first IEEE*. 2005.

12. Stella, P.M., S. DiStefano, M.D. Rayman, and A. Ulloa-Severino. "Early mission power assessment of the Dawn solar array," in *Proceedings of the Photovoltaic Specialists Conference (PVSC), 2009 34th IEEE*. 2009.
13. Brophy, J.R., G.B. Ganapathi, C.E. Garner, J. Gates, J. Lo, M.G. Marcucci, and B. Nakazono, "Status of the Dawn Ion Propulsion System," AIAA 2004-3433, 40th AIAA Joint Propulsion Conference, Fort Lauderdale, FL, July 11-14, 2004.
14. Personal Communication, Staley, M. and J. Waranauskas, Space Systems/Loral, Oct. 2010. Permission to publish granted.
15. Personal Communication, de Grys, K. and A. Mathers, Aerojet, Oct. 2010. Permission to publish granted.
16. Koch, B., A. Sultan, A. Mathers, and R.R. Hofer, "Development of a Modular Hall Thruster Power Converter," to be presented at the, 47th Joint Propulsion Conference, San Diego, CA, August 2011.
17. Brophy, J.R., J.W. Barnett, J.M. Sankovic, and D.A. Barnhart, "Performance of the Stationary Plasma Thruster: SPT-100," AIAA 92-3155, 28th Joint Propulsion Conference, Nashville, TN,
18. Sankovic, J.M., J.A. Hamley, and T.W. Haag, "Performance Evaluation of the Russian SPT-100 Thruster at NASA LeRC," IEPC 1993-094, IEPC, Seattle, WA, Sept. 1993.
19. Garner, C.E., J.R. Brophy, J.E. Polk, and L.C. Pless, "A 5,730-Hr Cyclic Endurance Test of the SPT-100," IEPC 1995-179, 24th International Electric Propulsion Conference, Moscow, Russia, Sept. 1995.
20. Garnero, P. and O. Dulau, "Alcatel Space Plasma Propulsion Subsystem Qualification Status," IEPC 2003-131, 28th International Electric Propulsion Conference, Toulouse, France, Mar. 2003.
21. Personal Communication, Danza, T., Space Systems/Loral, May 2010. Permission to publish granted.
22. Hofer, R.R., "High-Specific Impulse Operation of the BPT-4000 Hall Thruster for NASA Science Missions," AIAA 2010-6623, 46th Joint Propulsion Conference, Nashville, TN, July 25-28, 2010.
23. Sims, J.A., P.A. Finlayson, E.A. Rinderle, M.A. Vavrina, and T.D. Kowalkowski, "Implementation of a Low-Thrust Trajectory Optimization Algorithm for Preliminary Design," AIAA 2006-6746, AIAA/AAS Astrodynamics Specialist Conference, Keystone, CO, Aug. 21-24, 2006.
24. Cho, B., J. Davis, L. Hise, A. Korostyshevsky, G. Smith, A.V. Ley, P. Sharps, T. Varghese, and M. Stan. "Qualification testing of the ZTJ GaInP₂/GaInAs/Ge solar cell to the AIAA S-111 standard," in *Proceedings of the 34th IEEE Photovoltaic Specialists Conference (PVSC)*. 2009. Philadelphia, PA: IEEE.
25. Stan, M., B. Cho, B. Guzie, G. Smith, P. Sharps, and T. Varghese. "Air Force ManTech qualification of the 30% class GaInP₂/Ga(In)As/Ge solar cell to the AIAA S-111 standard: Results and recommendations," in *Proceedings of the 35th IEEE Photovoltaic Specialists Conference (PVSC)*. 2010. Honolulu, HI: IEEE.
26. Rauschenbach, H.S., *Solar Cell Array Design Handbook*, 1980, New York: Van Nostrand Reinhold. Section 2-33, Model 2.
27. Feynman, J., G. Spitale, J. Wang, and S. Gabriel, "Interplanetary Proton Fluence Model: JPL 1991," *J. Geophys. Res.*, 1993. **98**(A8): p. 13281-13294.
28. Kim, H.K. and C.Y. Han, "Analytical and numerical approaches of a solar array thermal analysis in a low-earth orbit satellite," *Advances in Space Research*, 2010. **46**(11): p. 1427-1439.